Astron. Astrophys. 283, 705–713 (1994)

ASTRONOMY AND ASTROPHYSICS

The GI2T interferometer on Plateau de Calern

D. Mourard[1], I. Tallon-Bosc[1], A. Blazit[1], D. Bonneau[1], G. Merlin[1], F. Morand[2], F. Vakili[1], and A. Labeyrie[2]

[1] Observatoire de la Côte d'Azur, Département Fresnel, URA 1361 du CNRS, F-O6460 Saint-Vallier de Thiey, France
[2] Laboratoire d'Astrophysique Observationnelle, Collège de France, F-06460 Saint-Vallier de Thiey, France

Received 3 August 1993 / Accepted 20 September 1993

Abstract. We describe in this article the current status of the "Grand Interféromètre à 2 télescopes" at the "Observatoire de la Côte d'Azur" in the south of France, near Grasse. After describing the 1.5 m telescopes and their control systems, we give details about the particular beam recombination and the focal instrumentation currently used. With the description of the data acquisition systems, we discuss the processing part of the GI2T work, which is presented in a subsequent article.

Key words: instrumentation: interferometers – telescopes

1. Introduction

After the pioneering work of A.A Michelson, the development of modern optical aperture synthesis can be traced back to the early seventies when interference fringes could be obtained with two separate telescopes 12 meters spaced apart (Labeyrie 1978). From the start the idea was to build an optical array, similar to radio-interferometers, with sub-milliarcsecond imaging capabilities on stellar and extra-galactic sources(Labeyrie 1976). Speckle interferometry had demonstrated that subapertures much larger than r_0, the sized "seeing" cells, could be exploited.

Following the initial work with a pair of 26cm telescopes, the I2T interferometer, it became apparent that useful astrophysical results could be obtained at visible and near-infrared wavelengths from interference fringes recorded from physically separated telescopes (Koechlin & Rabbia 1985; Thom et al.1986; DiBenedetto & Rabbia 1987).

At the same time, A. Labeyrie and his team undertook to build a larger instrument, the "Grand Interféromètre à 2 Télescopes" or GI2T, with a pair of 1.5m telescopes (Labeyrie 1978).

The principle of the GI2T is similar to the I2T: two independent Cassegrain-Coudé telescopes, movable on north-south tracks, feeding with 2 afocal beams an optical recombining system housed in a central laboratory (cf. Fig. 1). The recombiner can be translated between the two telescopes in order to compensate for the optical delay which, due to earth's rotation, varies as a function of hour angle.

Following the observation of the first fringes with the GI2T (Labeyrie et al.1986), an evaluation of the remaining problems for bringing this instrument up to an operational level was made. It appeared that three improvements were mandatory: the driving system of the spherical mounts, the recombination optics and the data processing system.

We describe here the present status of the GI2T, the first stellar interferometer operated in the multi-speckle mode with dispersed fringes. In addition to the current developments, we give details of performances for the different components of the instrument, i.e. the telescopes, the interferometric baseline control system, the optical recombination table, the photon-counting detector and the data acquisition system.

Another article devoted to the off-line data analysis and interferogram reduction procedures (Rigal et al.1993, in preparation) discusses a new method for estimating the absolute fringe visibility function, needed to obtain pertinent astrophysical parameters from the high-angular resolution measurements which can be carried out with the GI2T.

2. The GI2T telescope

2.1. Basic concept

The constraints for building optical telescopes for a long-baseline interferometer are severe. Each telescope must be easily movable in order to change rapidly the baseline. Its stellar tracking motion must not introduce variations in the optical path which might blur the interference pattern. It must continuously direct the outgoing stellar beams, named "Coudé beams", towards the central recombining system, and preferably with the highest optical throughput.

The new concept of spherical mount designed for the GI2T (Labeyrie et al.1986) responds to these constraints. The domeless "Boule telescope", made in concrete, is also very compact. With only three mirrors, it directs the horizontal afocal coudé beam towards the central station, requiring a special drive and system, more complex than in conventional telescopes (Mourard 1988).

In order to control the direction of the coudé beam, a rotation R_2 along the optical axis of the telescope is added to the basic diurnal rotation R_1. Thus, the direction of pointing is not

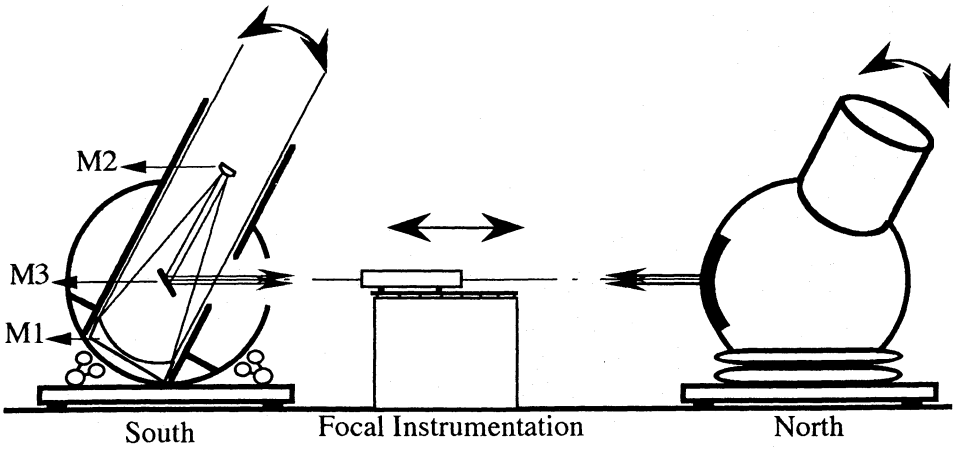

Fig. 1. Schematic layout of the GI2T Interferometer

changed but one direction of the coudé beam can be stabilized. By tilting (R_3) the plane tertiary mirror located at the centre of the sphere, it is possible to reflect a completely stabilized coudé beam in the direction of the central laboratory. The last motion is independent of the others since it is introduced by a small mechanism attached inside the telescope itself while the two main rotations act on the driving system of the spherical mounts. As the direction of the optical axis is always changing, the combination of the two rotations results in a complex rotation of the sphere around its centre, requiring control of its 3 angular degrees of freedom. The motion is equivalent to that of a horizontal yoke, such as used in the I2T.

2.2. Mechanical design

This complex motion is mechanically implemented by a large spherical bearing (Labeyrie 1982). The driving system is a ring supporting the sphere. This ring is motorized by three actuators (for three degrees of freedom) acting in three orthogonal directions within two different tangential planes. Motion of any of the three actuators results in a rotation of the sphere around its centre because the ring rolls on balls which themselves roll on a sphere concentric with the telescope (cf. Fig. 2). The rotation of the sphere being angularly limited, to about 1 degree corresponding to a drive time of 4 minutes, a second identical ring is needed to obtain a continuous motion with the two rings alternatively carrying the sphere. As one is driving the telescope, the second is going backwards to prepare for the next cycle. The telescope is therefore equipped with two sets of three small DC-motors plus three linears encoders. Their resolution of 1 micron is equivalent to 0.1 arcsecond on the sky, the sphere being 3.5 meters in diameter.

The clutching of the rings involves computer-controlled electrovalves and hydraulic pistons, carrying each of the 60 mm balls. These raise the rings by two millimeters to carry the sphere. Both spheres are made in reinforced concrete and the surface accuracy approaches one millimeter.

2.3. Attitude control

The information about the absolute attitude of the telescope is given by gravity encoders. A two axis pendulum equipped with incremental optical encoders having 4 arcseconds steps is installed inside each spherical shell. Due to mechanical imperfections and yet unsolved adjustment problems, the resulting accuracy of the pointing system is only 1 arcminute, but sufficient to acquire stars within the 3 arcminutes field of the pointing camera located at the prime focus of the telescope. The gravity encoders are well adapted to interferometric telescopes, which must move on the baseline whithout referring to a stable and fixed pier.

2.4. Optics

The diameter of the primary mirror is 1.52 meters and the focal ratio is 3. It is supported in its cell by three concentric pneumatic tubes with independently adjusted pressures for a correct mirror figure (Couderc 1932). The adjustment is not servo-controlled but is regulated in cosinus of the zenith angle and is manually corrected when necessary. It gives good results on both telescopes, where image quality is always dominated by the atmosphere (seeing of about 1 or 1.5 arcseconds on good nights).

The secondary hyperbolic convex mirror, 8 cm in diameter is set for an afocal combination. Then the reflected beam is directed along the optical axis towards the plane tertiary mirror, which can rotate along a perpendicular axis contained in its plane. The coudé beam is directed horizontally towards the focal laboratory. The diameter of the coudé beam is 75 mm corresponding to an optical magnification of 20.

15% of the incoming light is transmitted through the meniscus-shaped secondary mirror, then acting as a null lens, towards a CCD camera installed at the prime focus. With a field of view of 3 arcminutes and an angular resolution of about 1 arcsecond, it provides the coarse pointing of the telescope. Behind the secondary mirror, there is also a fiducial corner-cube reflector used to reflect to the backward face of the secondary mirror and then through the hole of the corner cube to the prime focus, the light of a laser coming from the central table

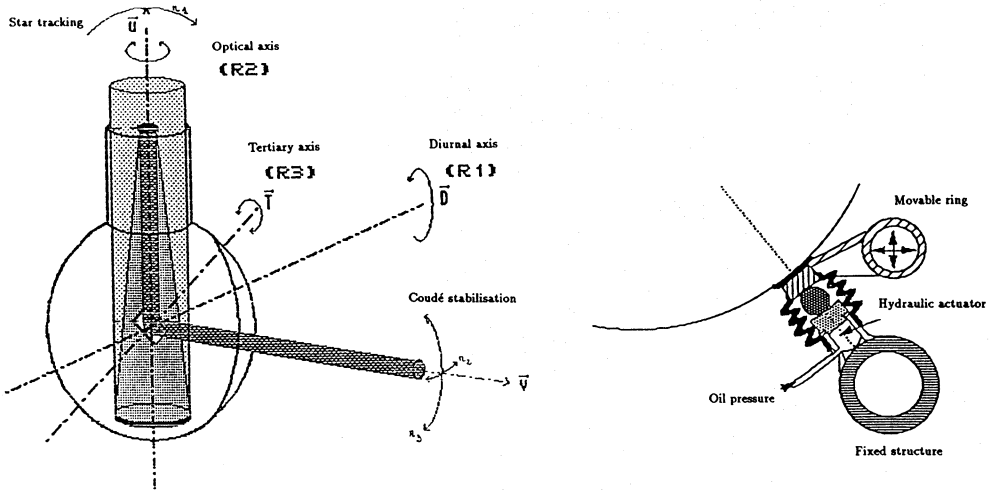

Fig. 2. Mechanical design of the spherical mount; driving and optical principle

(Labeyrie et al.1986). This laser beam materializes the inverse coudé direction from the central laboratory to the telescopes.

The secondary mirror, the CCD camera and the corner cube are rigidly mounted inside a tubular container, which can be translated axially for focus adjustments.

3. Control of the interferometer

3.1. Electronic and telescope software

Each telescope is driven by a complex electronic system, based on a 68000 microprocessor, programmed in assembler language. This system controls the eight encoders, drives the six motors, controls different systems on the telescope (rotation of the tertiary, electrovalve, primary camera, focus, pointing paddles, metrology system...) and communicates with the central computer placed in the central room of the interferometer. The communications utilize four RS232 lines through optical fibers. The telescope is not self-controlled, since its local 68000 microprocessor is not powerful enough to compute all the spherical equations. This task is done by the central computer, which sends every second of time the value of the different velocities to be applied to each actuator.

3.2. Optical path difference compensation

Part of GI2T's driving system is installed in a focal laboratory, at the coudé focus. An ICCD camera, with 2 fields of view, each 10x15 arcseconds, is used for the fine guiding of the telescopes. The pixel size on this camera is 0.05 arcsecond.

For the path difference compensation, the optical table rests on a moving carriage. The motion of this carriage is servo-controlled by a slave 68000 microprocessor with software in assembler and in C languages. It drives the table for the tracking of the fringes, using a torque motor and a tachometric generator, servo-controlled by means of a rotary incremental encoder, mounted on a driving screw. The pitch of the screw is 2 mm and the encoder provides a resolution of 10 nm.

The telescope positions along their railway tracks were measured initially with a commercial steel tape accurate within about 2mm. A new system recently installed uses a stainless steel perforated ribbon with an optical readout. The step of the perforated ribbon is 4 mm but the electronic encoding gives a resolution of 0.1 mm. This system is directly interfaced with the central computer via RS232 linkage. In both cases, the thermal dilatation of the ribbon is a critical problem. The solution currently adopted is to attach the ribbon at the centre of the focal station, as close as possible to the recombining prisms of the optical table and to stretch it at both ends. The thermal dilatation being homothetic in both arms, the fringe position is not affected, at least at the first order.

The metrology of the baseline is made only in the longitudinal direction. We assume that the lateral and vertical positions of the telescopes are invariant. This is not the case and it introduces some small but slow drifts of the interference fringes of about 100 μm per hour. Another consequence is a bad knowledge of the absolute position of both telescopes. Thus the scanning area is about 4 millimeters and, depending of intrinsic visibility and atmospheric conditions, the search of the fringes takes between 0 and 20 minutes.

3.3. Central control

The central computer is a master 68000 microprocessor using the OS9 operating system. Programmed in C language, it is first used for preparing the observations. The object and the configuration of the interferometer are chosen with a part of the FK5 catalog and the GI2T database. The main function of this computer is to supervise the central guiding of the GI2T. It generates the commands that are sent to both telescopes and to the optical carriage using eight serial lines. On the same bus as the central CPU, there is also a frame grabber board accepting four multiplexed video signals and having two serial ports. Three video inputs are used to control the field of the three guiding cameras of GI2T. This graphical board is driven by an original software, written on its 68020 microprocessor for the fine and completely automated guiding of the GI2T. The software is based on an online photocentre computation and uses the three following modes:

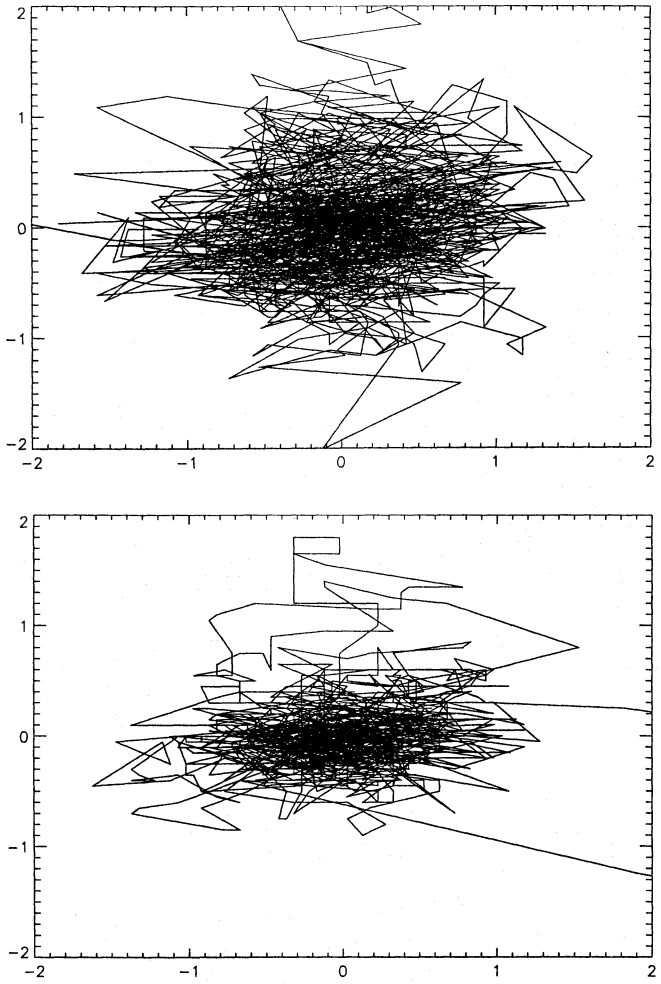

Fig. 3. Typical guiding sequence with the GI2T telescopes. Up, the south telescope, and down, the north telescope. RMS error is about 0.4 arcsec in both cases. Axis are graduated in arcseconds

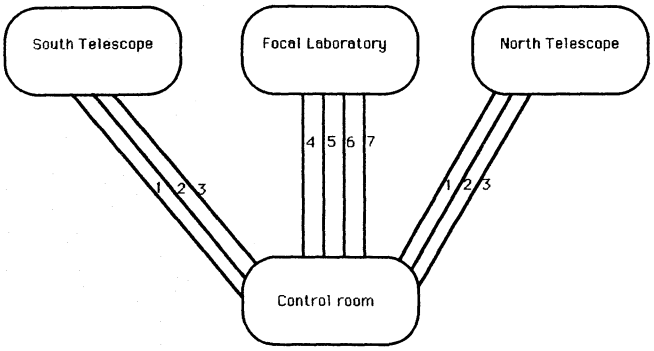

Fig. 4. General organisation of the signals communicated between the different parts of the GI2T interferometer. (1) is the optical fiber transmitting the video signal from the primary camera. (2) are the two optical fibers transmitting the 4 RS232 lines (Control of the telescope program, communication with the central computer, communication with the graphical computer, transmission of the metrological data). (3) is a cable which transmits different control signals (pointing "handset", focus of the telescope, manual motion of the tertiary mirror, on/off of the primary camera). (4) is the optical fiber which transmits the video signal from the ICCD Coudé camera. (5) is an optical cable which transmits either the video signals from the CP40 or the data from the CAR. (6) is the cable for the delay line control (RS232 for the control of the delay line program, RS232 for the communication with the central computer, RS232 for the communication with the fringe tracker system, time signal for the UT initialisation). (7) is a cable which transmits different control signals (on/off of the ICCD camera, manual adjustment of the ICCD gain, manual adjustment of the CP40 intensifier gains, on/off of the retro-reflected laser beam

pointing mode : the primary cameras are on, the coudé camera is off. The alignment laser is seen by the primary cameras and the photocenter errors, with respect to the nominal position, are translated in terms of coudé direction errors. Then, a rotation along the optical axis and a rotation of the tertiary mirror adjust the direction of the coudé beam.

guiding mode : the star is seen by the three cameras: the 2 primaries and the coudé ICCD. The error at the coudé field is used for the fine guiding of the star, while the error on the star position at the primary field is used for adjusting the coudé direction. Examples of typical guiding sequence are shown in Fig. 3.

repointing mode : during the change of ring, the star goes out of the coudé field but is still inside the primary field. The position errors are used for pointing corrections until the star appears again in the coudé field. Then we switch to the second mode.

The graphic board uses two dedicated serial lines for sending the position errors to the telescopes at a frequency of about 5 Hz, the time response of the telescopes being of the order of 0.5 s. The central computer uses three other serial lines to communicate with the three on-board microprocessors (south, north, table). Two other serial lines are used for communicating with the 0.1 mm metrology system. All serial lines are transmitted by optical fibers as well as all video signals coming from differents parts of the interferometer, in order to prevent electronic noisy interferences. Figure 4 summarizes this general organisation.

For managing the whole interferometer (2 telescopes, the focal carriage and the frame grabber computer), only one main program is necessary, owing to the multi-tasking capabilities of the OS9 operating system. Three background processes are running: one for all calculations (velocities of all 12 motors, control of the position of the four rings and decision for the simultaneous change of both telescopes in order to minimize the time gap due to the repointing of the stars, calculation of the converting matrices for the corrections...) and two for communicating with the telescopes. Another process is running for printing all the information and for communicating with the operator. A last one is running on the frame grabber processor for the photocentre determinations. All processes exchange information by using a common data-module.

3.4. Observing modes

It takes about 15 minutes for the whole initialisation of the interferometer. Due to the slow pointing of the telescopes, only 4 or 5 stars can be tracked during the night. For a given star, the observing time, which depends of the declination and the baselength, can reach 4 hours. It is also possible to use 4 consecutive baselengths on the star, the main limitation coming from the poor metrology. Only two persons are required for the operation: one for the general control (including the data acquisition), and one for the visual fine guiding of the interference pattern in the focal laboratory.

4. Beam recombination and focal instrumentation

4.1. Beam recombination

The beams coming from the telescopes are recombined in an image plane after reconfiguring the pupils, following the classical stellar Michelson technique. The fringed speckles are then dispersed and the spectra are recorded as short exposures on a photon counting detector before being recorded and processed (Labeyrie et al.1986). This spectral exploitation is a main particularity of the focal instrumentation of GI2T. A second unique feature is the size of the apertures, which provides a large collecting surface. But this advantage introduces also a difficulty in the dispersion mode. The light is indeed spread over one hundred or more speckles in the image ($\frac{D}{r_0} \geq 15$), the fringe pattern within each speckle being randomly phased. If the speckles are dispersed without having been separated before dispersion, the fringe pattern is blurred and its visibility is seriously decreased. Therefore, a slicing of the image at the entrance of the spectrograph is necessary (Bosc 1988, Bosc 1989).

Nevertheless, the dispersion mode has precious advantages, which explain why we prefer it to a set of filters: i) the continuous observation of the fringes across the spectral bandwidth; ii) the possibility to select a posteriori, during the data processing, different spectral channels for differential visibility measurements -for ex, in the continuum and in a spectral line-; iii) an easy means to servo-control the optical path difference (OPD) of the interferometer using the fact that the tilt of the fringes along the spectra, due to the proportionality between the fringe spacing and the wavelength, changes with the OPD (Bosc 1989). The last point is not the least since it allows a longer signal integration during the data acquisition.

To coherence an interferometer signifies that the beams always interfere at the position verifying a given OPD inside the coherence length (for ex. the zero OPD) between the beams coming from the telescopes. Because of the diurnal motion, this position is continuously moving along the north-south direction for GI2T, but it must be stable for the focal instrumentation during the observing time. To do that, the adopted solution consists in moving the focal instrumentation itself instead of having an auxiliary delay line. It simplifies the optical train but imposes limits on the weight and dimensions of the optical table. The motion, the speed of which increases with the hour angle, must be as smooth as possible, without any vibration which would make the observation of the fringes impossible. We tolerate a maximum amplitude of vibrations equal to 14 nm rms over 15 ms, corresponding to a 1% loss of visibility. Measurements made by P. Bourlon have shown that the vibrations increase beyond this level if the speed exceeds around 300 μm per second. The observing time is then limited to 2 hr in the worst case.

The optical table, schematically shown in Fig. 5, achieves essentially two functions, the second underlying the first: the observation of multi-speckle and polychromatic fringes on a detector (main beam) and the control of the necessary conditions for good acquisitions (auxiliary beams).

4.2. Acquisition of the fringes

The parallel coudé beams entering the recombiner are focused by an achromat, respectively at the south and north edges of the table. A second achromat followed by cemented prisms CP located at the centre of the table (cf. Fig. 5a) reconfigures the pupils and superimposes both images in the same plane I_1. The exit pupils become vertically aligned; their separation is equal, between centres, to 1.5 times the diameter of one pupil, thus fixing the number of fringes per speckle to 3. This value is the result of a compromise between a sufficient sampling of the fringes and a large number of recordable speckles, taking into account the limited number of pixels available on the detector (cf.Sect.5). The stability of the exit pupils is visually verified during the observation, as described in Sect.4.3.4. With the adopted pupil reconfiguration, the interference modulation is along the vertical direction. Therefore, the dispersion of the spectrograph must operate horizontally.

The entrance I_2 of the spectrograph is a series of slits, as explained before. The principle of the "image slicer" is the following (see Fig. 5b): a set of glass wedges Wp of different angles and same width, which corresponds to one speckle, splits the image I_2 and deflects vertically the beams corresponding to different slices. These slices are imaged on the top of each other on the detector (I_3) using a set of adjustable mirrors Mp located between the grating and the last achromat (Fig. 5b). The spectrograph has three interchangeable gratings on a turret, as needed for the varied observational programs. The spectral resolutions $\Delta\lambda$ and bandwidths BW are: $\Delta\lambda_1$=.15nm for BW_1=36nm; $\Delta\lambda_2$=.4nm for BW_2=80nm and $\Delta\lambda_3$=1nm for BW_3=170nm.

Spectral source (Ne, He, Ar) can illuminate the spectrograph for its calibration (AxB_1): their light is introduced in the main beam by translating a right-angle prism Pc (see Fig. 5). Furthermore, we can create a flat field calibration on the detector with two yellow light emitting diodes Le, which are each located behind a diffuser, Df, 30 cm in front of the camera.

A grid can also be imaged on the latter in order to calibrate the geometrical distorsion of the whole optical train, from the slit, plus the camera. Using the same auxiliary beam as the spectral calibration, a white-light source filtered by a Fabry-Perot FP is inserted into the spectrograph and provides an horizontal modulation in the spectrum. An additional vertical modulation, providing a grid-like spectrum, is given by a mask in front of I_2.

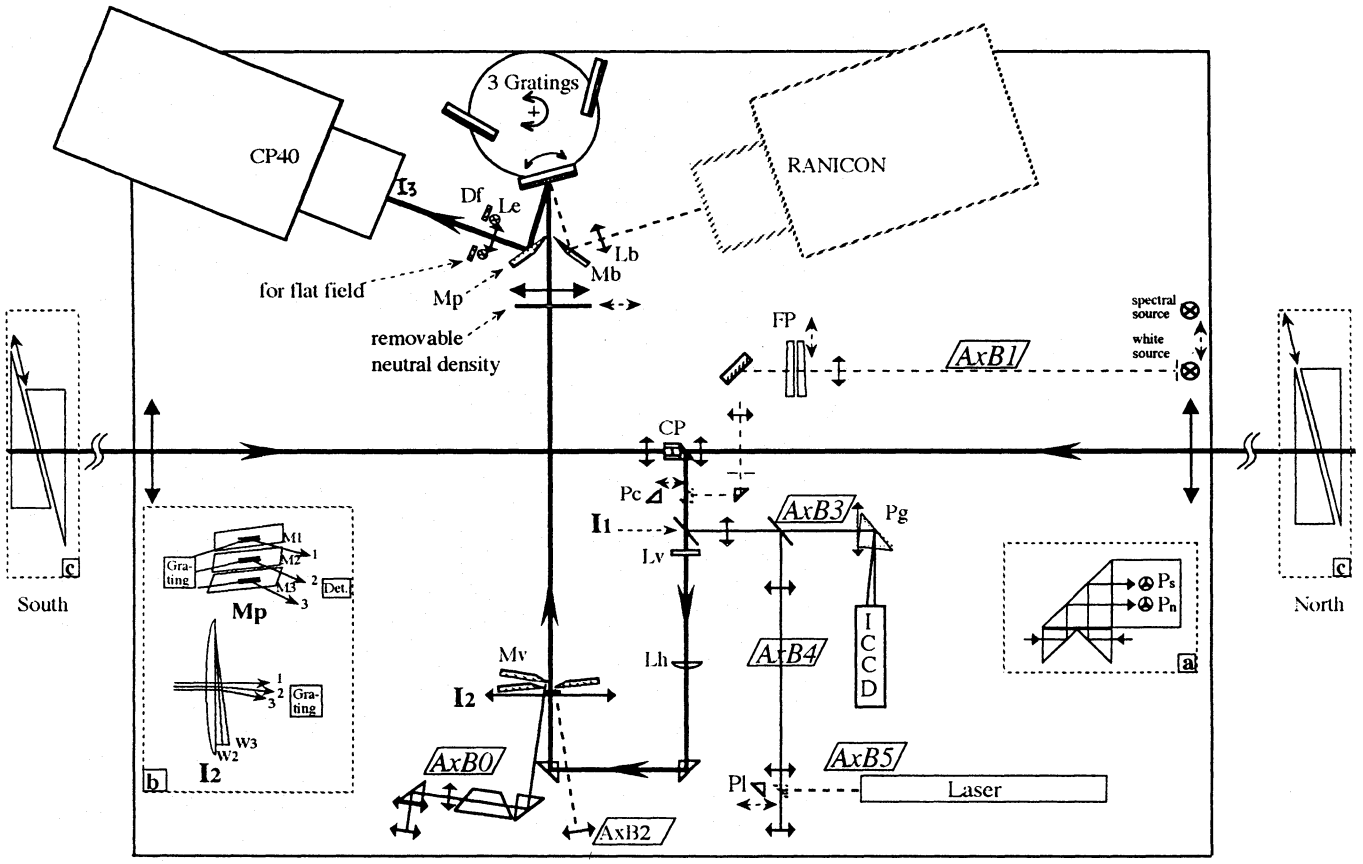

Fig. 5. Schematic view of the optical table showing the main beam for recording the multi-speckle and dispersed fringes, and the auxiliary beams useful to control the acquisitions. Some details are also drawed: a. the recombining element for reconfiguring the pupil and so fixing the fringe spacing. b. the principle of the "image slicer" with its two elements: a series of 10 wedges (only 2 represented) of different angles sticked on a field lens in I_2 slices the image whereas, in the pupil plane next to the grating, a set of adjustable mirrors images the slices on the top of each other. At the present time, only two slices are in operation. c. The compensating system of the atmospheric dispersion: the presence of a glass thickness in the smallest arm of the interferometer (the south side for the figure, as in Fig. 1), compensates the longer path through the air of the other coudé beam

$I_1$and I_2 are conjugated through two crossed cylindrical lenses Lv and Lh, an anamorphic system which results in $\frac{\gamma_v}{\gamma_h} = 10$, for optimizing the sampling of the dispersion, as well as the fringe spacing (Bosc 1989). In spite of this anamorphosis and the small number of fringes per speckle, it is impossible to record the dispersed speckle pattern across the full spectrum due to the insufficient number of pixels of existing photon counting detectors. Currently, the image-slicer operates with two slices only.

A third slice of the image I_2 is however utilized as the entrance slit of the so-called "visual spectrograph" (AxB_0) serving for the detection and the guiding of the fringes, as described in the next section.

For observations with the highest spectral dispersion, it is possible to record simultaneously two separate spectral domains on two detectors, as shown by Fig. 5: for example, the Hα region of the dispersed fringe pattern can be imaged on the CP40 detector while a mirror Mb collects the part of the spectrum centred on the line Hβ and sends it through an achromat Lb towards the RANICON detector.

4.3. Adjustments of the interferometer

4.3.1. Fringe tracking (AxB_0)

A plane mirror (Mv in Fig. 5) just behind I_2 intercepts the third slice of the image and directs it towards a low-dispersion visual spectroscope ($\Delta\lambda$=1.5nm for a bandwidth BW=400nm). This spectroscope provides a signal for an observer who looks continuously at several dispersed speckles and scans until the fringes are detected. Then, the observer monitors the motion of the optical table by keeping the tilt of the fringes as constant as possible, parallel to a reticle (cf.Sect.3.2). Such a method for tracking limits obviously the practical visual magnitude of GI2T, to only 4 or 5, depending on the turbulence conditions and the intrinsic visibility of the fringes.

4.3.2. Visualisation of the entrance of the spectrograph (AxB_2)

The external edges of the image slicer in I_2 are plane mirrors, serving to direct into an eyepiece the light missing the entrance

slits of the spectrograph. It allows to visually verify the centering of the images on the slits of the spectrographs.

4.3.3. Guiding of each telescope (AxB_3)

In I_1, a non-coated pellicle beamsplitter takes 10% of the light to form two separated images on a single detector, an ICCD camera (cf. Sect. 3.2). In order to achieve this, each pupil is imaged on a separate right-angle prism Pg. A differential rotation angle between both prisms allows the separation of both images. A field diaphragm on I_1 delimits the coudé guiding field (10"x15").

4.3.4. Visualisation of the exit pupils (AxB_4)

A second beamsplitter implemented in AxB_3 reflects part of the guiding beams towards lenses and an eyepiece allowing the visual control of the geometry for both exit pupils. Those must be on a common vertical line at a fixed position and spacing. An unstable geometry of the exit pupils affects the acquisition of interferometric data and degrades the visibility of the fringes.

4.3.5. Telescope alignment during the pointing phase (AxB_5)

Using a push-pull right-angle prism Pl which crosses AxB_4, an He-Ne laser beam, installed on the table, can be projected in the focal intrumentation. It goes through the recombining optics back to the cameras at prime foci. In service during the pointing phase, when the motion of the telescopes is fast, this auxiliary beam helps keeping the coudé beams aligned.

4.3.6. Compensation of the atmospheric dispersion effect

In general, the optical paths through the air of the horizontal arms of the interferometer are unequal. This difference of paths could be represented for the beams of the longer arm by the crossing of a parallel "air-plate" if the whole interferometer were in vacuum. Because the refractive index of air varies with the wavelength, this air plate causes a chromatic effect on the recombined images, similar to a dispersion effect. On the fringe pattern dispersed by the spectrograph, this effect materializes as curvature of the fringes, which decreases their visibility and degrades the signal-to-noise ratio.

A well-known but approximate correction method consists in inserting a compensating glass thickness in the shortest arm. The value of the thickness depends on the stellar object and varies temporally. The system adopted in the GI2T, currently under completion, is a doublet of prismatic plates mounted head to tail on each arm (see Fig. 5c). The motion of the glass wedges either side of their mean position will allow to minimize the reduction of fringe curvature for every observation and also to easily change the glass thickness during one observation when necessary (Bosc 1989).

Other causes of visibility degradation, like the field rotation, are not currently dealt with. The present optical table is still a prototype, pending a new version which is now under study.

5. Photon counting detectors and data acquisition

Presently two different types of photon-counting detectors are used on the GI2T: a RANICON camera (Clampin et al.1988), and a 2 stage intensified CCD detector called CP40 (Blazit 1987). As explained in section 4.2.1, the spectrograph projects two dispersed interferograms on the detector. In order to record these interferograms, which are arranged vertically, one would ideally need about 1000 vertical pixels to sample correctly the fringe modulation of the dispersed speckle patterns. The horizontal number of pixels is defined by the number of spectral channels that one wishes to record simultaneously. The CP40, with its 4 CCD chips of 288x384 pixels each, matches these characteristics. The RANICON detector provides only 400x400 theoretical pixels, but can better freeze the atmospheric effects with its 100 μs time resolution. It is potentially of interest on blue or violet wavelengths.

5.1. The RANICON detector

This camera, built at the Space Telescope Science Institute under the direction of F. Paresce, uses a resistive anode technology with a proximity 3-stage Z-type microchannel plate intensifier (Clampin et al.1988). The front cathode is a S20, 25mm in diameter and cooled by Peltier elements. The ion-barrier has been suppressed on it for a higher primary quantum efficiency attaining in principle 0.2. The X-Y coordinates are computed on 9 bits each by a hardwired electronics board. The useful detecting area has a circular format with 400 pixels across. The time-tagged XY coordinates are sent on a 32 bit parallel interface, with the 12 highest bits corresponding to the time coordinate, presently limited to a 100 μs resolution, and the adequate handshaking flags. The XYT streams are transmitted through a 32 bits FO linkage interface between the central laboratory and the control room. They can be read simultaneously by a real-time fringe processor (Koechlin 1992) and by a 68020-based OS9 computer for recording the observational data. During the observation, the latter can display the XYT photon-events on a CCIR TV monitor, like the video signal from a standard CCD camera. This helps adjusting the optics. The digital recording is made through the local network on DAT magnetic tapes.

The detective quantum efficiency of the RANICON is less than 0.05 in the red. The readout electronics saturate beyond 20000 photon-events/s. The local dead-time per pixel is not known yet, but it should not differ from other resistive anode detectors, i.e. between 40 and 50 ms, whilst the effective spatial resolution has not been evaluated yet. Theoretically, the RANICON should present several advantages with respect to cameras such as the CP40: the distortion is smaller and the signal is read in a simple format of XY-time coordinates. The latter can be used a posteriori to optimize the correlation time of short exposures in order to overcome the loss of fringe visibility due to the speckle lifetime. The moderate resolution of photon-events arriving in spatio-temporal proximity is a potential problem of resistive anodes for uses as interferometry: for such uses, the most

important information is obtained from close pairs of events, in space and time.

5.2. The CP40 detector

This photon counting detector, built by A.Blazit and R. Foy (Blazit & Foy 1988), has been available part-time on the GI2T for 5 years. The CP40 is a 2-stage intensified photon-detector, with output on a mosaic of 4 Thomson 288x384 CCD's which are readout at the standard rate of 20 ms. The input stage is a 40 mm first generation VARO intensifier with a red extended S20 photocathode. The fiber-optics output phosphore screen P20 of this intensifier is coupled to an RTC 50 mm second generation intensifier which has also a P20 output screen and 4 fiber-optics tapers for coupling the CCDs. The multiplication gain of the first stage is 60, further amplified 50,000 times the RTC tube for a total gain of $3x10^6$. These CCD's are full-frame chips, with 23x23 μm pixels, representing 52x52 μm on the input photocathode. The front photo-cathode of the VARO intensifier is cooled by liquid nitrogen to -20°C but the minimum dark current is already attained at -15°C. In these conditions, the residual dark count does not exceed 10 photon-events per 20 ms frame and per CCD chip. There is about 1 ion-event per 20 ms frame and per CCD chip, but these events are partially rejected by the photon-centroiding electronics, and their persistent track can be discarded by off-line processing of the raw data.

The CP40 output signal consists of four standard 20 ms video signals, clamped by a single pixel clock in order to synchronize the 4 video signals. These signals are transmitted by means of FO cables towards the GI2T control-room, and fed to 4 separate on-line hardwired centroiding processors. The video signals are digitized by an 8 bits ADC. The photocentres are computed over a 3x3 pixels matrix following classical centroiding algorithms specially adapted to the CP40 by A. Blazit. The digital X-Y coordinates of each photon-event are computed on 11 bits, but experience shows that the physical spatial resolution matches the size of the CCD pixels. The 4 sets of X-Y coordinates are grouped on a single digital format of 24 bits, where 2 bits are used to specify the number of the CCD channel. These 24 bits are written by means of a DMA interface directly in the RAM memory of a 68020-OS9 computer, through the VME-VSB bus. Actually, the DMA interface adds a 4th byte to the 3 bytes per photon (24 bits for XY and the CCD channel), set to hexadecimal FF when addressing the photons inside a same 20 ms short frame. These frames are separated in time by setting the first byte of a new 20 ms image to a positive value. The photon-buffers are transferred by an SCSI interface on a 1.2 Gbyte hard-disk and recorded on a DAT magnetic tape or transferred through the network on Hewlett Packard type 9000/710 workstations. Calibrations of the pincushion distortion and of uniform sensitivity are made before reducing the data (Thiebaut & Foy 1993).

6. Concluding remarks

The GI2T interferometer, now in routine operation, is a complex machine. The data processing methods utilized will be presented in a second article (Rigal et al.1993). The current outcome of the GI2T encourages us to think about increasing its performances in order to optimize the observations and to expand the scientific program. Collaboration with astrophysicists authors of theoretical star models are under way for selecting objects and for interpreting the results. The current scientific program includes different classes of objects: Be stars like γCas, βLyr and oAnd; Luminous Blue Variables like PCyg; eclipsing binaries like βAur and resolved bright stars of known angular diameter like αLyr and αCyg, for calibrating externally the instrument.

This program is restricted by the low limiting magnitude currently achieved, due to the visual detection and tracking of the fringes and to the lack of a continuous metrology accurate within microns. Therefore, steps have been taken towards an automated interferometer, usable on fainter objects and capable of measuring low-visibility fringes. The main developments are an absolute metrology system using laser beams and polychromatic fringe counting, an automated fringe tracking and an upgraded focal instrumentation.

A prototype of a laser tridimensional absolute metrology system designed for the O.V.L.A. project (Labeyrie et al.1992) is under development on the north arm of the GI2T (Morand et al.1992). Three laser beams are focused from the focal laboratory onto a corner cube retroreflector located at the centre of the tertiary mirror of the telescope. Interferometric techniques are used to measure the length of these three beams. In order to obtain absolute measurements, two lasers are used simultaneously. A laser diode provides a large spectral bandwidth of about 20 nm while an He-Ne gas laser gives two spectral lines. The fringes obtained with the laser diode are dispersed and their slope is measured by determining the position of the high frequency peak in the power spectrum of the fringe pattern. This position gives the OPD between laser beams and reference beams but with a low accuracy. By measuring the phase of the fringes in both gas laser lines and by applying a fractional fringes algorithm, we reach an accuracy of a few fringes. Then, beams lengths are calculated and a triangulation gives the tridimensional position of the centre of the tertiary mirror. Laser beams are dynamically pointed and optical path differences are automatically controlled by moving small delay lines. First tests on short baselines show that the sensitivity is about 0.2 microns for longitudinal distance measurements and 2 microns for transverse measurements. This metrology system must be duplicated on the south arm before being completely operational.

In parallel, an automated stellar fringe tracker has been developed by L. Koechlin at Toulouse Observatory. His system processes in real-time the data recorded by the time-tagged RANICON photon detector through the main beam (Koechlin 1992). The application of a Fast Fourier Transform algorithm on successive frames makes the tracking of the fringes possible if the fringe peak is detected after a short delay ($\simeq$4s). The initial tests have been encouraging.

Finally, the study of a new optical table has begun. The recombining optics will provide different functions, currently missing, like the compensation of the field rotation, an automated pupils stabilisation, the use of the whole speckles in the image. It should also include, on each arm, a simplified unit of adaptive optics, based on the system developed by F. Roddier (Roddier 1988). The aim is to concentrate the light in a central bright speckle, avoiding the present slicing of the image and providing a significant gain of the signal-to-noise ratio. Furthermore, the optical table will dispose of a third arm in order to receive the beams coming from a third telescope, currently built by A. Labeyrie and his group at Collège de France for the O.V.L.A project (Labeyrie et al.1992).

Acknowledgements. We wish to thank R. Foy and E. Thiebaut for the use of the CP40 detector and of its acquisition and pre-processing software. Many thanks are also due to M. Dugué, P. Antonelli and P. Bourlon from the "Groupe Projet" of the "Observatoire de la Côte d'Azur" for the mechanical and software improvements of the focal carriage. We thank finally J. Pinel and the colleagues of the technical group at the Calern Observatory for their invaluable help.

References

Blazit, A.,1987, Ph.D. Thesis, Univ. of Nice.
Blazit, A. and R. Foy, 1988, Journal des Astronomes Français, 32, April, p21.
Bosc, I., 1988, Proc. Coll. "High Resolution Imaging by Interferometry I.", Ed. Merkle F., ESO, Garching 1988, 735.
Bosc, I., 1989, Ph.D Thesis, Univ. of Nice.
Clampin, M., Crocker, J., Paresce, F. and Rafal, M.,1988, Review of scientific instruments, 59, 8 Part I, 1269.
Couder, M., A., Ph.D. Thesis, Faculté des Sciences de Paris, (1932).
DiBenedetto, J.P. and Rabbia, Y., 1987, A&A, 188, 114.
Koechlin, L. and Rabbia, Y., 1985, A&A., 153, 91.
Koechlin, L., 1992, Proc. Coll. "High Resolution Imaging by Interferometry. II.", Ed. Merkle F., ESO, Garching 1991, 1239.
Labeyrie, A. 1975, ApJ, 196, L71.
Labeyrie, A. 1976, in Progress in Optics, Ed. E. Wolf, p49.
Labeyrie, A., 1978, ARA&A, 16, 77.
Labeyrie, A. 1982, Sky and Telescope, April, p334.
Labeyrie, A., Schumacher, G., Dugué, M., Thom, C., Bourlon, Ph., Foy, F., Bonneau, D. and Foy, R., 1986, A&A., 162, 359.
Labeyrie, A., Cazalé, C., Gong, S. et al, 1992, Proc. Coll. "High Resolution Imaging by Interferometry. II.", Ed. Merkle F., ESO, Garching 1991, 765.
Morand, F., Gong, S., Mourard, D. and Labeyrie, A, 1992, Proc. Coll. "High Resolution Imaging by Interferometry. II.", Ed. Merkle F., ESO, Garching 1991, 1227.
Mourard, D., 1988, Proc. Coll. "High Resolution Imaging by Interferometry. I.", Ed. Merkle F., ESO, Garching 1988, 729.
Mourard, D., Bosc, I., Labeyrie, A., Koechlin, L. and Saha, S., 1989, Nat, 342, 520.
Rigal, F., Bonneau, D., Mourard, D., Tallon-Bosc, I. and Vakili, F., 1993, submitted to A&A.
Roddier, F., 1988, Appl. Opt. 27, 1223
Thiebaut, E. and Foy, F., 1993, submitted to A&A.
Thom, C., Granès, P., and Vakili, F., 1986, A&A., 165, L13

This article was processed by the author using Springer-Verlag LaTeX A&A style file version 3.